Cellular and Molecular Life Sciences

RESEARCH ARTICLE

The p38/MAPK pathway regulates microtubule polymerization through phosphorylation of MAP4 and Op18 in hypoxic cells

Jiong-Yu Hu · Zhi-Gang Chu · Jian Han ·
Yong-ming Dang · Hong Yan · Qiong Zhang ·
Guang-ping Liang · Yue-Sheng Huang

Abstract In both cardiomyocytes and HeLa cells, hypoxia (1% O_2) quickly leads to microtubule disruption, but little is known about how microtubule dynamics change during the early stages of hypoxia. We demonstrate that microtubule associated protein 4 (MAP4) phosphorylation increases while oncoprotein 18/stathmin (Op18) phosphorylation decreases after hypoxia, but their protein levels do not change. p38/MAPK activity increases quickly after hypoxia concomitant with MAP4 phosphorylation, and the activated p38/MAPK signaling leads to MAP4 phosphorylation and to Op18 dephosphorylation, both of which induce microtubule disruption. We confirmed the interaction between phospho-p38 and MAP4 using immunoprecipitation and found that SB203580, a p38/MAPK inhibitor, increases and MKK6(Glu) overexpression decreases hypoxic cell viability. Our results demonstrate that hypoxia induces microtubule depolymerization and decreased cell viability via the activation of the p38/MAPK signaling pathway and changes the phosphorylation levels of its downstream effectors, MAP4 and Op18.

Introduction

Microtubules (MTs) are a major component of the eukaryotic cytoskeleton and have been assigned many functional roles, such as intracellular trafficking, protein synthesis, intracellular signaling, chromosome segregation during mitosis and cell fate determination [1, 2]. MTs are also involved in specific myocardial cell functions, including regulation of contraction, ion channel function, receptor recycling, and sarcomere structure [3–7].

Hypoxia is a common pathological process in many diseases. It plays a key role in tumor cell survival, invasion, and metastasis. Myocardial hypoxia is relevant not only to patients with coronary artery disease experiencing repetitive ischemia [8] but also to patients with obstructive sleep apnea, hypertensive heart disease, cardiomyopathy, or severe burns [9, 10]. Cytoskeletal damage, including MT alterations, has been linked with various pathological conditions. Disruption of the MT network has been reported in ischemia as an early ultrastructural change correlated with the cellular reaction to a metabolic challenge [11–13], and irreversible cell damage may be associated with the collapse of the MT cytoskeleton [14]. Proliferation of the MTs with taxol has been reported to protect against hypoxia/re-oxygenation injury [15], whereas the MT disruptor, colchicine, has been shown to abolish the protective effect of ischemic pre-conditioning [16, 17]. However, there are some conflicting reports, for example, in breast carcinoma cells, hypoxia (3% O_2 for 24 h) stimulates carcinoma invasion by stabilizing MTs [18].

J.-Y. Hu and Z.-G. Chu contributed equally to this work.

J.-Y. Hu · Z.-G. Chu · Y. Dang · H. Yan · Q. Zhang ·
G. Liang · Y.-S. Huang (✉)
State Key Laboratory of Trauma, Burns and Combined Injury,
Institute of Burn Research, Southwest Hospital,
The Third Military Medical University,
400038 Chongqing, People's Republic of China
e-mail: yshuang.tmmu@gmail.com

J. Han
Department of Gynecology and Obstetrics, Daping Hospital,
The Third Military Medical University,
400038 Chongqing, People's Republic of China

The transition between the stable and disassembled MT forms is regulated by two main classes of MT regulators: MT-associated proteins (MAPs), which have the ability to polymerize and stabilize MTs [19], and Oncoprotein 18 (Op18)/stathmin family members, especially the MT-destabilizing protein families [20]. MAPs are good substrates for many protein kinases in vitro [21], and their phosphorylation was shown to reduce the ability of MTs to polymerize in vitro [22]. MAPs include tau and MAP2, which are expressed abundantly only in nervous tissue, and MAP4, expressed ubiquitously in non-neuronal cells [23]. The phosphorylation state of MAP4 is thought to be a key factor in the regulation of MT stability. Op18/stathmin is a widely expressed and highly conserved cytosolic phosphoprotein [24]. It forms complexes with α/β-tubulin heterodimers and destabilizes MTs in vivo and in vitro by promoting MT disassembly [25]. The MT-destabilizing activity of Op18/stathmin is turned off by phosphorylation [26–29]. It is widely recognized that a balance between MT-stabilizing and -destabilizing factors regulates the dynamics of MT polymerization and that the phosphorylation of these factors is important for alterations to MT dynamics [30].

The protein kinase systems involved in MAP4 and Op18/stathmin phosphorylation include members of the cyclin-dependent kinase family (CDKs) [26], microtubule affinity regulating kinase (MARK), mitogen-activated protein kinase (MAPK) [27], CAM kinase II [28], and PKA [29], and so on. It has been reported that hypoxia (1% O_2) induced a rapid and time-dependent activation of p38/MAPK activation [31, 32], and that p38/MAPK could modulate MT dynamics through phosphorylating MAPs [33] and Op18 [27]. What is more, pharmacological inhibition of p38/MAPK by SB203580 attenuated nocodazole-induced MT depolymerization [34]. Accordingly, we have focused on p38/MAPK and observed its function in hypoxia-induced MT disruption.

Although the function of MAP4 and Op18 phosphorylation in regulating MT dynamics suggests crucial roles for these molecules during hypoxia, little is known about their phosphorylation changes or the molecular mechanism(s) triggered by hypoxia. Here, we describe the hypoxia-induced phosphorylation changes of MAP4 and Op18, and report the identification of a p38/mitogen-activated protein kinase (p38/MAPK) pathway that plays an important role in regulating MAP4 and Op18 phosphorylation during hypoxia. We found that hypoxia (1% O_2) led to MT disruption after treatment for 15 min in HeLa cells, but this disruption was delayed until after 30 min in cardiomyocytes (CMs). Our results suggest that in both CMs and HeLa cells the hypoxia-activated p38/MAPK pathway initiates MT disruption and alters cell viability by phosphorylating the downstream effector MAP4 and dephosphorylating Op18.

These results provide novel insights into the pathogenic mechanisms of MT disruption during hypoxic disease.

Materials and methods

Cell culture and hypoxia treatment

All animal procedures have been approved by the Institutional Animal Care and Use Committee of the Third Military Medical University and followed the Principles of Laboratory animal care (NIH publication). Neonatal rat ventricular CMs were prepared according to McMillin et al. [35] using 1- to 3-day-old Sprague–Dawley rats. CMs were plated at 5×10^6 cells/60-mm dish and maintained for 48 h in DMEM/F12 with 5-bromodeoxyuridine (BrdU; 31 mg L^{-1}), 10% (V/V) heat-inactivated fetal bovine serum (FBS), penicillin G (100 U ml^{-1}), and streptomycin (100 mg ml^{-1}) before hypoxia treatment. HeLa cells were cultured in RPMI-1640 under standard mammalian cell conditions. The p38/MAPK inhibitor, SB203580 (5 μM), or an equal volume of vehicle (dimethyl sulfoxide) were added to these cultures and incubated at 37°C for 30 min before hypoxia.

Hypoxia treatment was performed according to previous methods [36]. Briefly, hypoxic conditions were achieved by using an anaerobic jar (Mitsubishi, Tokyo, Japan) and vacuum glove box (Chunlong, Lianyungang, China). The serum-free medium was placed in the vacuum glove box filled with a gas mixture of 94% N_2, 5% CO_2, and 1% O_2 overnight and allowed to equilibrate with the hypoxic atmosphere. Cells were subjected to hypoxic conditions by replacing the normoxic medium with the hypoxic medium plus either SB203580 or the vehicle solution and then placed in the anaerobic jar.

MKK6(Glu) recombinant adenoviruses construction and transduction

To assess the effects of signaling proteins, we constructed a recombinant adenovirus that expressed the mutated, constitutively activated human mitogen-activated protein kinase kinase 6 (MKK6). MKK6 phosphorylates p38/MAPK on Thr-180 and Tyr-182, which activates p38/MAPK; overexpression of constitutively activated MKK6 can selectively and constitutively activate p38/MAPK [37, 38]. The pcDNA3 MKK6(Glu) plasmid, which expressed constitutively activated MKK6, was developed from the Addgene plasmid 13518, by R. Davis, University of Massachusetts, Worcester, MA [37], and the recombinant adenoviruses were prepared using the AdMax™ system (Microbix, Ontario, Canada) according to the instructions. The transgene expression in CMs and HeLa cells was tested by western blotting.

CMs were maintained in DMEM/F12 and 10% FBS, and HeLa cells were maintained in RPMI-1640 and 5% FBS. The medium was changed to medium without FBS, and infected with adenoviruses at a multiplicity of infection of 100–200 particles/cell for 24–48 h. The cells were then cultured in DMEM/F12 or RPMI-1640 with 10% FBS before morphological or biochemical analysis.

Immunostaining

Cells were plated on laminin-coated glass coverslips and cultured as described above. Cells were then immersion-fixed in 4% paraformaldehyde for 20 min, permeabilized with 0.1% Triton X-100 in PBS for 20 min, and then blocked in 10% goat serum for 1 h. To observe the MT structure, mouse anti-α-tubulin primary antibodies (1:100, SC5286; Santa Cruz, CA, USA) were diluted with PBS + 5% goat serum and coverslips incubated at 4°C overnight. Coverslips were washed in PBS, followed by incubation with goat anti-mouse secondary antibodies conjugated to fluorescein isothiocyanate (FITC; 1:1000; Sigma-Aldrich, St. Louis, MO) or cyanine 3 (Cy3; 1:1000; Beyotime, Shanghai) for 1 h at 37°C. The nuclei were then stained for 2 min with 4′, 6′-diamidino-2-phenylindole (DAPI; 0.5 μg/ml; Sigma-Aldrich). Cells were imaged with confocal microscopy (TCS-NT; Leica, Wetzlar, Germany).

Extraction and quantification of tubulin fractions

Polymeric and monomeric tubulin fractions were isolated using a method previously described by Putnam et al. [39]. Briefly, cells grown in 60-mm dishes were washed twice with a MT stabilization buffer (MTSB, 37°C) containing 0.1 M piperazine-N,N'-bis (2-ethanesulfonic acid, pH 6.8) (Pipes), 2 mM ethylene glycol-bis (β-aminoethylether) N,N,N',N'-tetraacetic acid (EGTA), 0.5 mM $MgCl_2$, 20% glycerol, and a protease inhibitor cocktail (Sigma-Aldrich). Cells were incubated with MTSB + 0.1% Triton X-100 for 30 min, and the supernatant collected as the monomeric tubulin fraction. The Triton X-100 insoluble fraction, corresponding to the polymerized tubulin, was then solubilized in a RIPA lysis buffer (Sigma-Aldrich) with 2 mM phenylmethylsulfonyl fluoride (PMSF) and a protease inhibitor cocktail. Polymeric and monomeric tubulin fractions were quantified using western blot analysis.

Western blot analysis

Free and polymerized tubulin fractions prepared in the above section were probed with anti-α-tubulin (1:200; Santa Cruz) antibody; GAPDH (1:1000; Sigma-Aldrich) in the supernatant was chosen as the internal control for free tubulin and VDAC (1:1000; Abcam, MA) in the Triton

X-100 insoluble fraction was chosen as the control for polymerized tubulin. Whole cell lysates were prepared and analyzed by western blot using primary antibodies to p38 (1:1000; Cell Signaling Technology, Beverly, MA), phospho-p38 (1:1000, Thr180/Tyr182; Cell Signaling Technology), MAP4 (1:2000; BD Biosciences, San Jose, CA), phospho-MAP4 (1:200, Ser768; Biolegend, San Diego, CA), Op18 (1:1000; Sigma–Aldrich) and phospho-Op18 (1:200; Ser16; Santa Cruz). As a loading control, GAPDH was probed and visualized. Immunocomplexes were visualized and quantified with an enhanced chemiluminescence detection kit (Amersham Pharmacia, Piscataway, NJ), using horseradish peroxidase-conjugated secondary antibodies (1:2000; Santa Cruz).

Immunoprecipitation

To show the phospho-p38 and MAP4 complex formation, cells (60 mm dish) were lysed in 300 μl RIPA buffer with 2 mM PMSF and a protease inhibitor cocktail. Anti-phospho-p38 (Thr180/Tyr182; Cell Signaling Technology) or anti-MAP4 (BD Biosciences) antibodies were incubated with 150 μL cell lysate for 6 h at 4°C after which the complexes were precipitated with protein A/G-Sepharose (Santa Cruz) overnight at 4°C, the precipitates washed 3 times with PBS at 0°C, then probed with anti-MAP4 or anti-phospho-p38 antibodies using western blotting.

Cell viability assay

Cell viability was determined using a cell counting kit (CCK-8; Dojindo Molecular Technologies, Kumamoto, Japan). CCK-8 is a colorimetric assay for the determination of the number of viable cells by producing a water-soluble formazan dye upon reduction in the presence of an electron carrier using tetrazolium salt WST-8 ($n = 6$) [40, 41]. The experiment was repeated three times.

Statistical analysis

Data are expressed as $\bar{X} \pm SD$. SPSS 11.0 was used for statistical analysis and significance evaluated by one-way ANOVA followed by post-hoc tests. P values ≤ 0.05 were considered statistically significant.

Results

Hypoxia-induced microtubule depolymerization

HeLa cells subjected to 15 min of hypoxia showed clear signs of MT disruption and modification. The normal relatively orderly pattern of staining became disrupted and less

regular and some breakages in the MT network were apparent. There was some shrinkage in the vicinity of the nuclei and along the edges of the cell (presumably attached to the coverslip) such that the MTs appeared to curl and buckle (see Fig. 1) compared to normal cells, which have relatively straight MT segments. Disruption continued with additional time under hypoxic conditions so that by 30 min there was a significant decrease in MT density and a loss of MTs closely adjacent to the plasma cell membrane; after 60 min only a thin and disordered residual MT network, with some MT fragments, remained (lower panel, Fig. 1a). The higher magnification inserts in the micrographs of Fig. 1 illustrate the presence of broken microtubules induced by hypoxia. In neonatal rat CMs, hypoxia also led to MT breakages and shrinkage, which was similar to that in the HeLa cells. However, the loss of MTs closely adjacent to the plasma cell membrane and the reduction of MT density were not as significant as that observed in HeLa cells at equivalent levels of hypoxia (upper row, Fig. 1a).

The tubulin fractions were isolated and analyzed by western blot in order to further clarify the changes in tubulin form [39]. Our results confirmed a time-dependent decrease in polymerized tubulin with a parallel increase in free tubulin in CMs and HeLa cells after hypoxia (Fig. 1b). In HeLa cells, the polymerized tubulins significantly decreased and the free tubulins significantly increased after hypoxia for 15, 30, or 60 min. In contrast, there were no significant changes in CMs after 15 min of hypoxia, although polymerized and free tubulin fractions significantly changed after 30 and 60 min of hypoxia.

Effect of hypoxia on MAP4 and Op18 phosphorylation

Given the importance of phosphorylation in accommodating MAP4 and Op18 activities, we investigated the effects of hypoxia with anti-phospho-MAP4 (Ser768) and anti-phospho-Op18 (Ser16) antibodies (Fig. 2). Western blot and quantitative analyses of normoxic control cells revealed that, in HeLa cells and CMs, MAP4 phosphorylation remained at a low basal level, and Op18 phosphorylation remained at a high basal level. Hypoxia led to an increase in the expression of phosphorylated MAP4 following 15 min of hypoxia that reached a plateau by 30 min and was still evident after 60 min of hypoxia. Concomitant with the increase in phosphorylated MAP4 was a reduction in phosphorylated Op18 that was also apparent after 15 min of hypoxia. The expression of MAP4 and Op18 did not change significantly by 60 min of hypoxia.

Hypoxia activated p38/MAPK signaling pathway

To elucidate further the signaling events involved in the hypoxia-induced effects on MT structure, we investigated the activation of p38/MAPK by hypoxia. Phosphorylated (Thr180/Tyr182) and activated p38/MAPK were tested by immunoblotting with a phosphor-specific p38/MAPK antibody (Fig. 3). Hypoxia induced phosphorylation of p38/MAPK was significantly elevated by hypoxia for 15 min with a 1.6-fold increase in HeLa cells and 2.7-fold increase in CMs and remained elevated throughout the 60 min of hypoxia.

Effect of p38/MAPK pathway on microtubule dynamics

To test whether activation of p38/MAPK signaling is necessary for MT disruption, we treated the cells with the p38/MAPK inhibitor, SB203580 (5 μM). In both CMs and HeLa cells (Fig. 4a), SB203580 could abolish the MT depolymerization induced by hypoxia (1% O_2 for 30 min). Furthermore, quantification of polymeric tubulin levels confirmed that in CMs and HeLa cells, SB203580 (5 μM) treatment significantly increased the polymeric tubulin in hypoxia-treated cells (Fig. 4b). We then overexpressed MKK6(Glu), a constitutively activated p38 kinase activator, using recombinant adenoviruses expressing constitutively activated MKK6 and GFP. In both CMs and HeLa cells (Fig. 5a), control cells (left panel) and cells expressing GFP (middle panel) showed no changes in MT dynamics. In contrast, transduction with MKK6(Glu) (right panel) resulted in very significant MT depolymerization. Quantification confirmed that the polymeric tubulin levels in the MKK6(Glu) group decreased significantly. These results suggest that the p38/MAPK pathway plays an important role in promoting microtubule disassembly.

Involvement of the p38/MAPK pathway in hypoxia-induced MAP4 phosphorylation and Op18 dephosphorylation

To study the mechanism of p38/MAPK signaling in regulating hypoxia-induced dynamic MT changes, we measured phospho-MAP4 and phospho-Op18 with or without the p38/MAPK inhibitor SB203580 and MKK6(Glu) recombinant adenovirus by western blot analysis.

In CMs (left panel, Fig. 6), under hypoxic conditions (1% O2 for 30 min), SB203580 treatment resulted in a significant decrease in phospho-MAP4 and an increase in phospho-Op18. Under normoxic conditions, treatment of SB203580 resulted in a significant increase in phospho-Op18, but no change in phospho-MAP4 compared to the control group. In HeLa cells (right panel, Fig. 6), SB203580 treatment resulted in a significant phospho-MAP4 decrease and a phospho-Op18 increase under normoxic and hypoxic conditions.
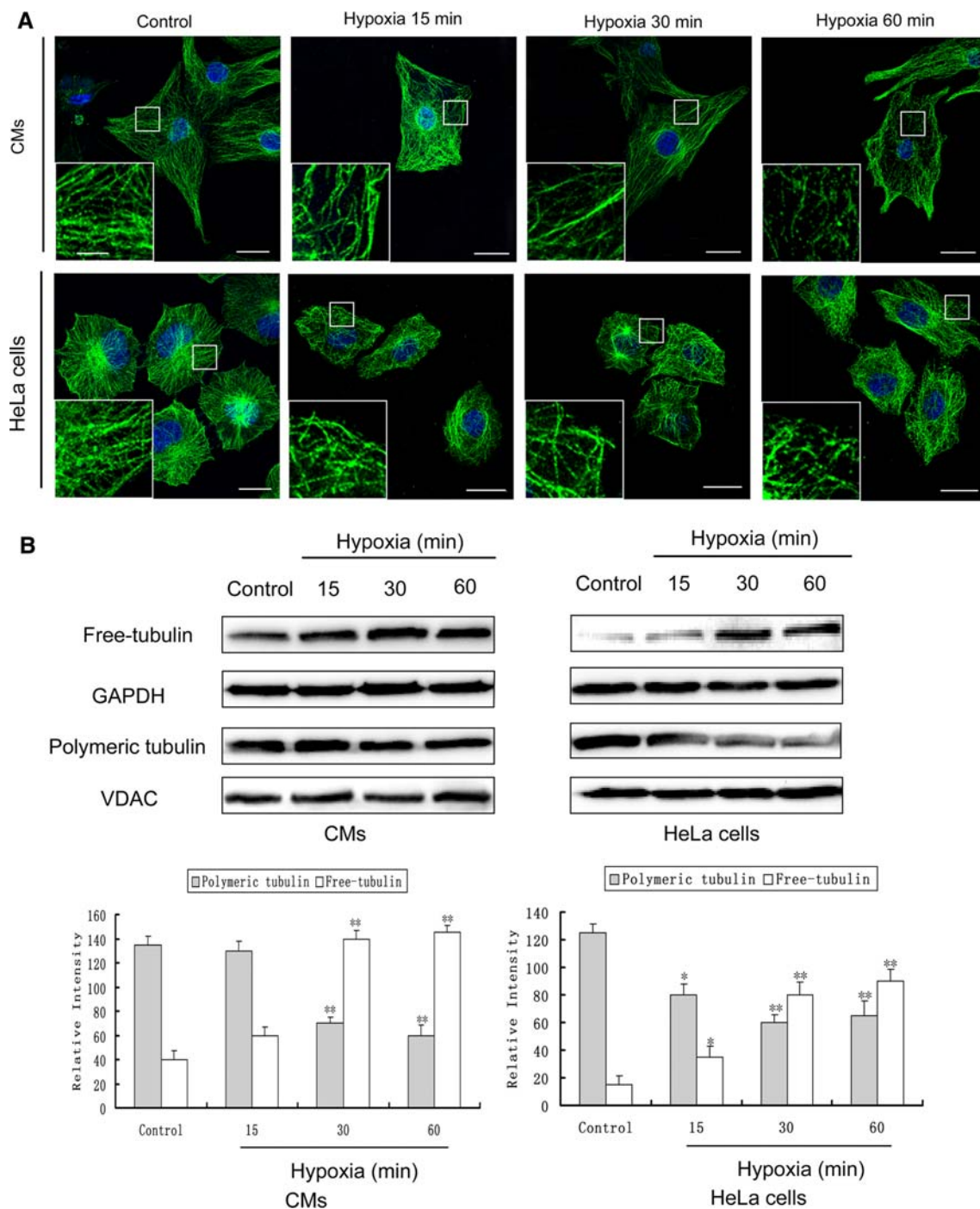
Fig. 1 Hypoxia-induced microtubule depolymerization. Immunofluorescent confocal micrographs and immunoblot analysis of microtubule dynamics in neonatal rat cardiomyocytes (*CM*s) and HeLa cells. **a** Micrographs of CMs and HeLa cells, showing control cells and cells after 15, 30, and 60 min of hypoxia. All the cells were stained for α-tubulin (*green*) and the nuclear stain DAPI (*blue*). *Bar* 25 μm. The *boxed areas* are shown at higher magnification in the *inserts* to illustrate details of MTs. *Bar* 6 μm. The immunoblots in (**b**) were prepared from CMs and HeLa cells. Free and polymerized tubulin fractions were prepared and probed with anti-α-tubulin antibody; GAPDH in the cytosol fractions was chosen as the internal control for free tubulin and VDAC in mitochondrial fractions was chosen as the control for polymerized tubulin. *Graph* represents the relative integrated signal from densitometer readings for three separate experiments. The data represent the $\bar{X} \pm \mathrm{SD}$ ($n = 3$). *$P < 0.05$, **$P < 0.01$ versus controls, one-way ANOVA followed by Tukey comparison tests

Fig. 2 Effect of hypoxia on MAP4 and Op18 phosphorylation. Western blot analysis of phospho-MAP4 (p-MAP4), MAP4, phospho-Op18 (p-Op18) and Op18 in neonatal rat CMs and HeLa cells under normoxic and hypoxic conditions. Representative western blots are shown for the two groups. *Graph* represents the $\bar{X} \pm SD$ ($n = 3$) of the relative integrated signals. $*P < 0.05$, $**P < 0.01$ versus controls
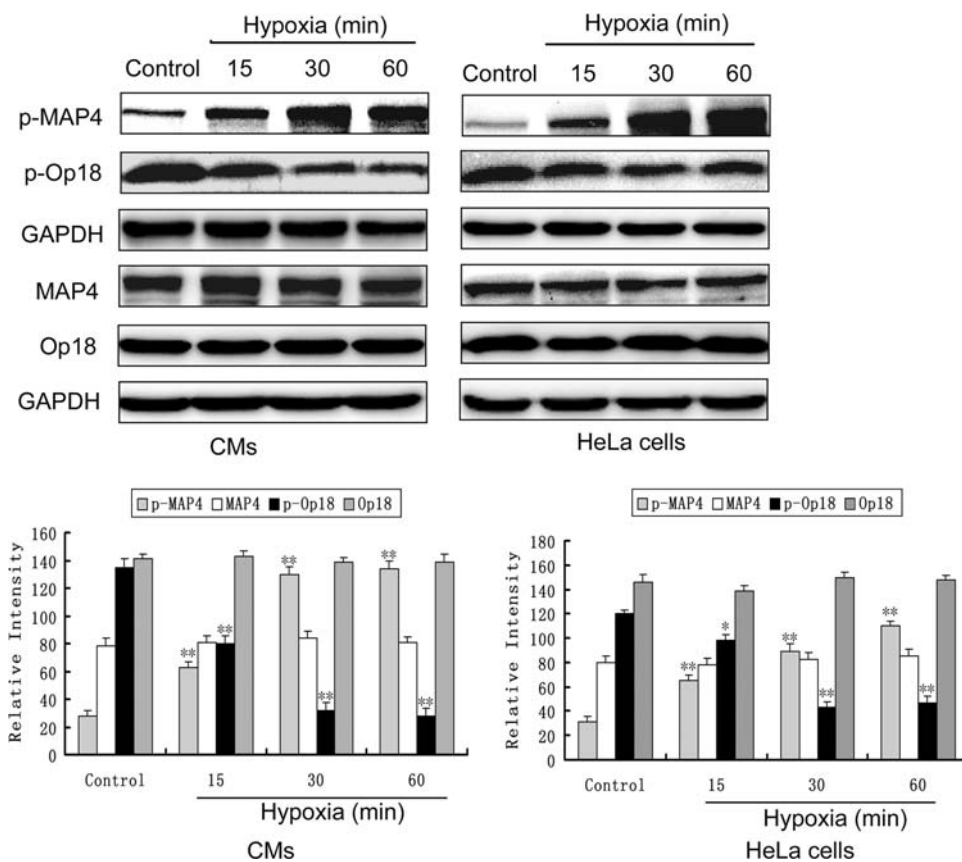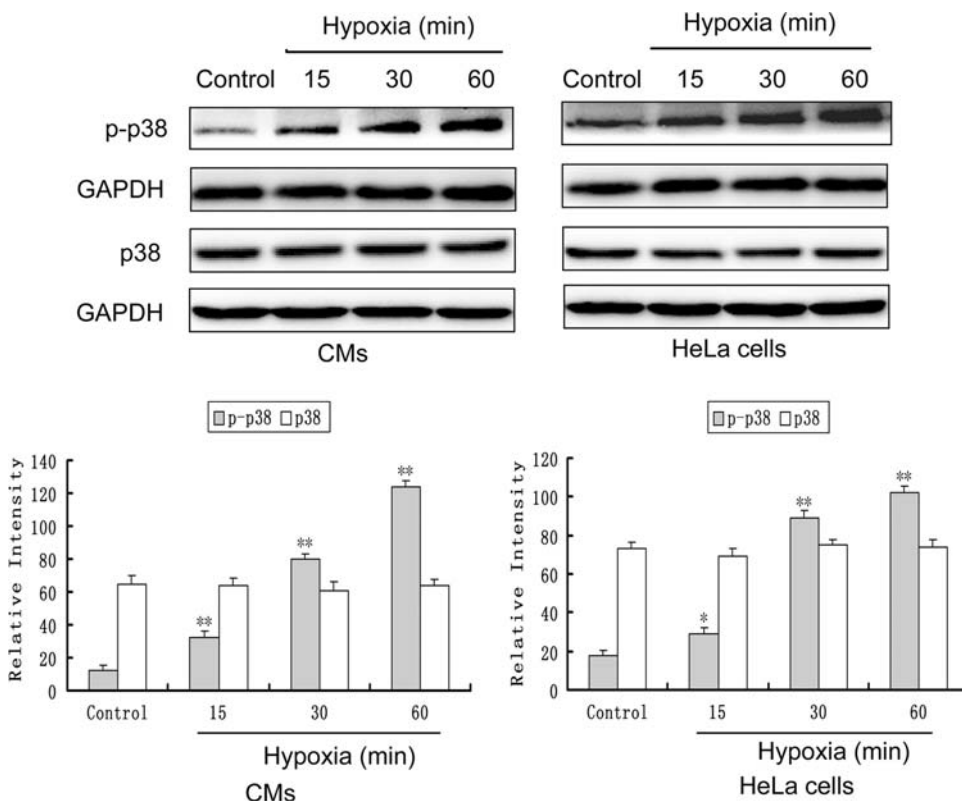
Fig. 3 Hypoxia activated p38/MAPK signaling pathway. Representative blots and data summary of phospho-p38 (p-p38) and p38 in CMs and HeLa cells under normoxic and hypoxic conditions. Representative western blots are shown for the two groups. *Graph* represents the $\bar{X} \pm SD$ ($n = 3$) of the relative integrated signals $*P < 0.05$, $**P < 0.01$ versus controls
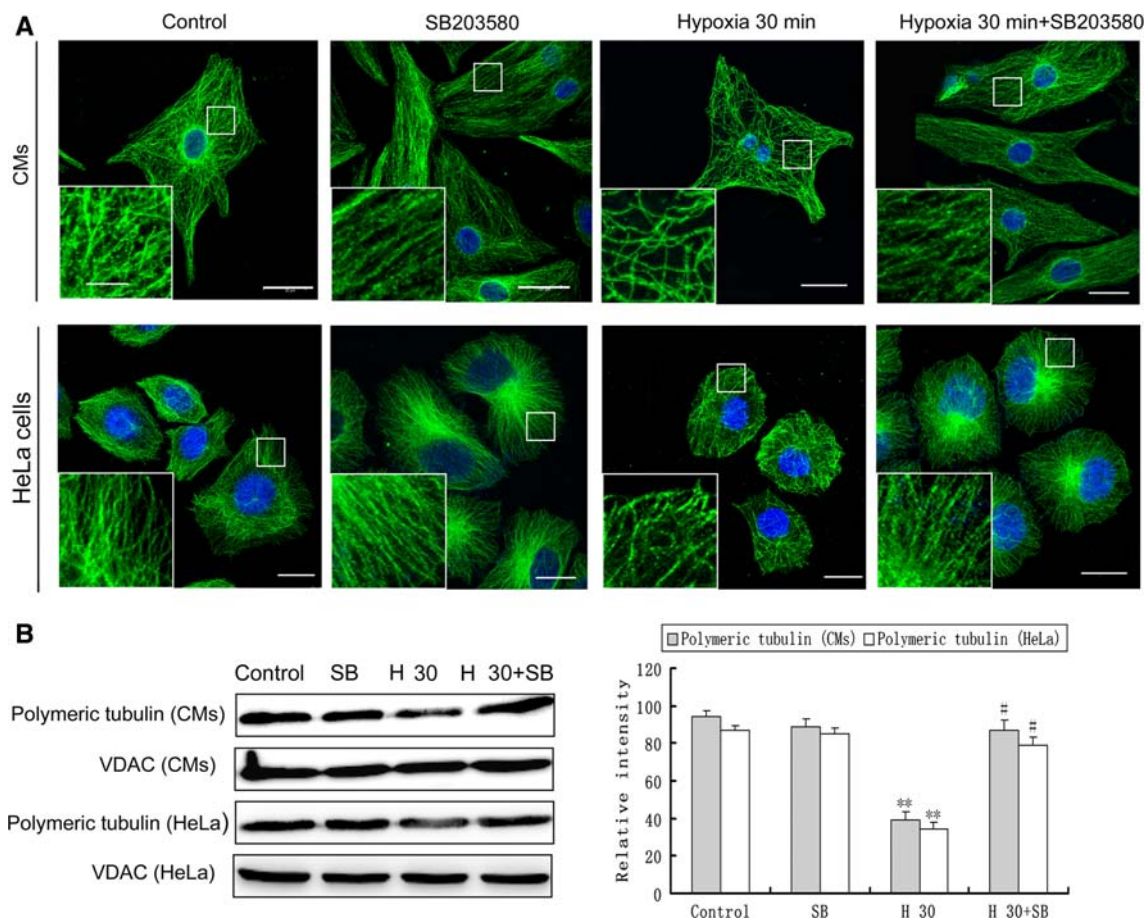
Fig. 4 Effect of the p38/MAPK inhibitor, SB203580, on the morphology and quantification of MT dynamics in HeLa cells and neonatal rat CMs. **a** Immunofluorescent confocal micrographs of CMs and HeLa cells under normoxic and hypoxic [1% O_2 for 30 min (H 30)] conditions with and without the addition of SB203580 (*SB*). Cells were stained for α-tubulin (*green*) and with DAPI for the nuclei (*blue*). *Bar*, 25 μm. The *boxed areas* are shown at higher magnification in the *inserts* to illustrate details of MTs. *Bar* 6 μm. **b** Immunoblots of CMs and HeLa cells. Polymerized tubulin fractions were prepared and probed with an anti-α-tubulin antibody, and VDAC was used as a standard control. *Graph* represents the $\bar{X} \pm SD$ ($n = 3$) of the relative integrated signals. *$P < 0.05$, **$P < 0.01$ versus controls

The effects of overexpressing MKK6(Glu) on the phosphorylation of MAP4 and Op18 are shown in Fig. 7. Overexpression of MKK6(Glu) resulted in a 6- and 4-fold increase in the basal level of phospho-p38 and a 3- and 4-fold increase in MAP4 phosphorylation in CMs and HeLa cells, respectively. At the same time, overexpression of MKK6(Glu) resulted in a significant decrease in the basal level of Op18 phosphorylation in CMs and HeLa cells. It suggested that activated p38/MAPK could phosphorylate MAP4 and dephosphorylate Op18.

The interaction between phospho-p38 and MAP4

A possible mechanism for hypoxia activated p38/MAPK is that it forms a complex when in contact with MAP4; we tested this hypothesis using immunoprecipation. In both CMs and HeLa cells (Fig. 8), MAP4 was co-immunoprecipitated with phospho-p38 (left panel) and conversely,

phospho-p38 co-immunoprecipitated with MAP4 (right panel) under nomoxic and hypoxic (1% O_2 for 30 min) conditions. The amount of MAP4 and phospho-p38 complexes in the hypoxia group was higher compared to the normoxic group, which suggests that the interaction between phospho-p38 and MAP4 increased after hypoxia.

Cell viability

In initial experiments, we found that both hypoxia and the microtubule-destabilizing chemotherapeutic agent colchicine reduced cell viability, but pretreatment with the microtubule-stabilizing chemotherapeutic agent, paclitaxel (Taxol), enhanced the survival of hypoxic CMs. Based on these observations, we hypothesized that the p38/MAPK inhibitor, SB203580, and MKK6(Glu) transduction, which influenced MAP4 and Op18 phosphorylation and MT dynamics, would increase cell viability. Results of a CCK-8

Fig. 5 Effect of MKK(Glu) overexpression on the morphology and quantification of MT dynamics in HeLa cells and neonatal rat CMs. **a** In the immunofluorescent confocal micrographs all the cells were divided into control, GFP transduction and MKK6(Glu) transduction groups and were stained for α-tubulin (*red*) and the nuclear stain DAPI (*blue*). *Bar*, 25 μm. The *boxed areas* are shown at higher magnification in the *upper inserts* to illustrate details of MTs. *Bar* 6 μm. The *lower inserts* show the cells containing GFP after transduction (note the lack of staining in the control group). *Bar* 25 μm. **b** Immunoblots of cardiomyocytes and HeLa cells. Polymerized tubulin fractions of the cells were prepared and probed with anti-α-tubulin antibody, and VDAC was used as a control. *Graph* represents the $\bar{X} \pm$ SD ($n = 3$) of the relative integrated signals. *$P < 0.05$, **$P < 0.01$ versus controls
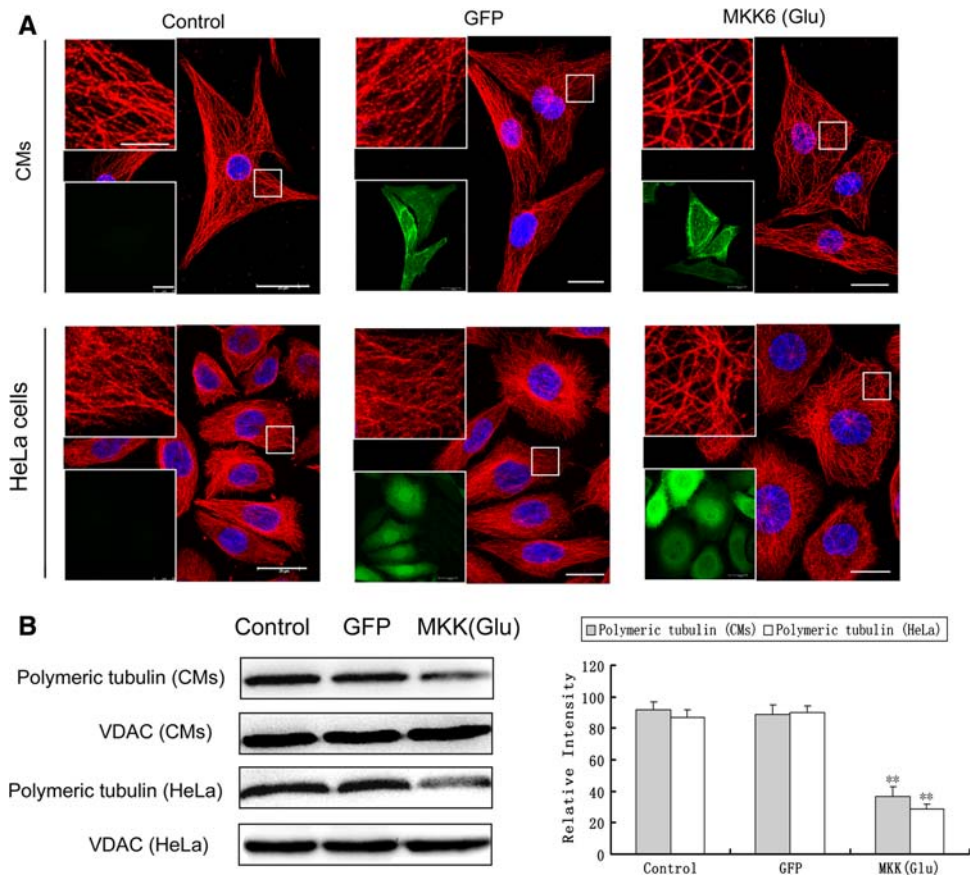

Fig. 6 Involvement of SB203580 in hypoxia-induced MAP4 phosphorylation and Op18 dephosphorylation. Western blot analysis of phospho-MAP4 (p-MAP4), MAP4, phospho-Op18 (p-Op18) and Op18 of CMs and HeLa cells in the presence or absence of the p38/MAPK inhibitor SB203580 (5 μM, SB) under normoxic and hypoxic (1% O_2 for 30 min, H 30) conditions. Cell lysates were immunoblotted with antibodies that recognize p-MAP4 (Ser768), MAP4, p-Op18 (Ser16), Op18 and GAPDH. A representative western blot is shown. *Graph* represents the $\bar{X} \pm$ SD ($n = 3$) of the relative integrated signals. *$P < 0.05$, versus controls; #$P < 0.05$, versus H 30 group
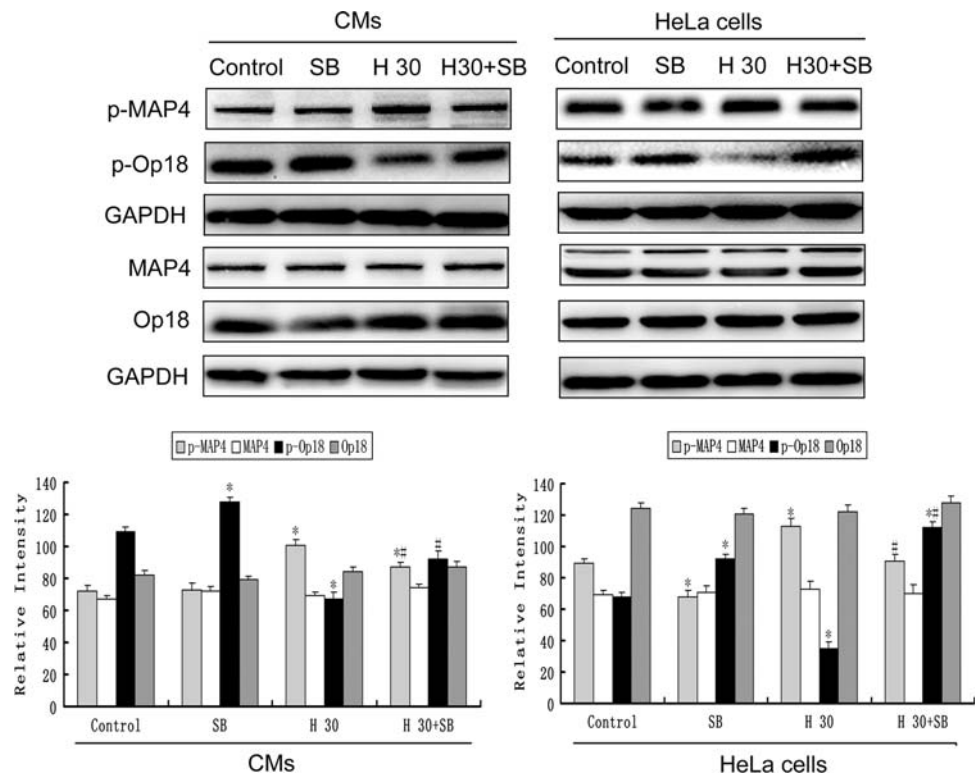
Fig. 7 Involvement of MKK6(Glu) in hypoxia-induced MAP4 phosphorylation and Op18 dephosphorylation. CMs and HeLa cells were divided into control, GFP transduction and MKK6(Glu) transduction groups. Cell lysates were immunoblotted with antibodies that recognize phospho-MAP4 (p-MAP4; Ser768), MAP4, phospho-Op18 (p-Op18; Ser16), Op18 and GAPDH. A representative western blot is shown. *Graph* represents the $\bar{X} \pm SD$ ($n = 3$) of the relative integrated signals. $*P < 0.05$, versus GFP group
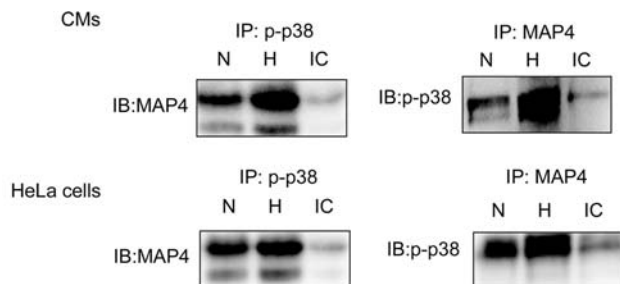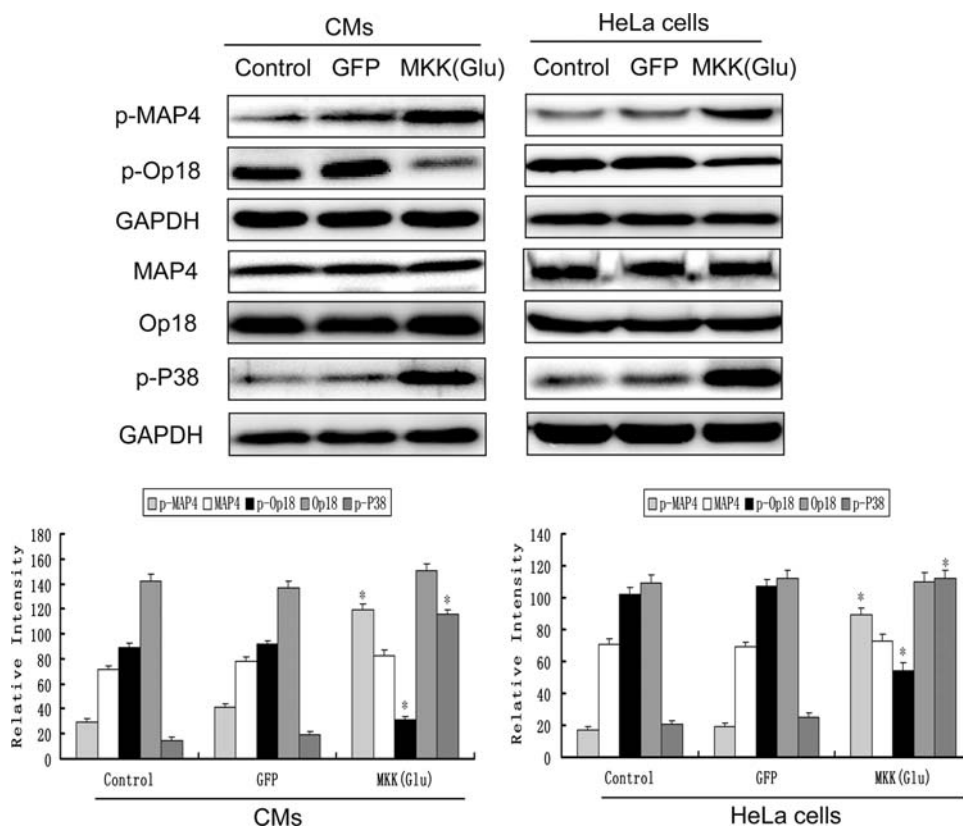
Fig. 8 The interaction between phospho-p38 (p-p38) and MAP4 detected by immunoprecipitation under normoxic (*N*) and hypoxic [1% O$_2$ for 30 min (H)] conditions. The representative blots were immunoprecipitated by anti-phospho-p38 and anti-MAP4 antibodies in CMs and HeLa cells and then immunoblotted with anti-MAP4 or anti-phospho-p38 antibody. *IP* Immunoprecipitation, *IB* immunoblotting, *IC* isotype control

assay in CMs and HeLa cells treated with or without SB203580 and MKK6(Glu) transduction are illustrated in Fig. 9; cell counts are based on colorimetric assays.

Hypoxia decreased cell viability in HeLa cells (right panel) and CMs (left panel), but pretreatment with SB203580, dramatically increased cell survival; there was no significant difference between the control and SB203580 treated groups under normoxic conditions. In contrast, MKK6(Glu) transduction decreased cell viability in HeLa cells and CMs under normoxic and hypoxic conditions (experiments were replicated three times). These

results suggest that pretreatment with SB203580, the p38/MAPK inhibitor, improved the survival of CMs and HeLa cells exposed to hypoxia, while MKK6(Glu) transduction reduced cell viability.

Discussion

Although MT disruption is a common phenomenon in hypoxia-induced cell injuries and is closely connected with CM dysfunction, very little is known about how hypoxia leads to MT depolymerization. In addition to heart disease, hypoxia plays an important role in tumor proliferation and migration, which is also closely connected with MTs. In both CMs and cancer cells, MAP4 is the major MAP subtype. Therefore, in order to make our observations more generally applicable with respect to MAP4 and Op18 phosphorylation in hypoxia-induced MT disruption, we used CMs and HeLa cells. HeLa cells, an immortal cell line originally derived from cervical cancer cells, are one of the most common cell lines used in MT research [42, 43].

The present study demonstrates that the MAP4 and Op18 phosphorylation status plays a critical role in MT dynamics. We show that hypoxia causes phosphorylation of MAP4 and dephosphorylation of Op18 and reveal a hitherto unexplored pathway by which hypoxia-activated p38/MAPK phosphorylates the down-stream effector
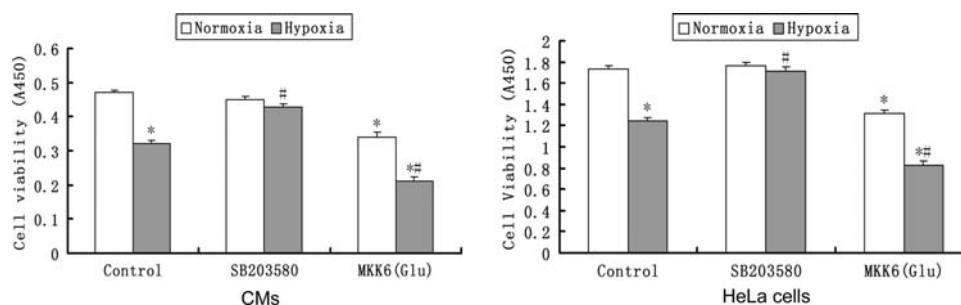
Fig. 9 Cell viability. CMs and HeLa cells were pretreated with the p38 inhibitor SB203580 (5 μM) or MKK6(Glu) overexpression and then subjected to 30 min of hypoxia. *Graph* represents the $\bar{X} \pm$ SD ($n = 6$) of the relative integrated signals. *$P < 0.01$, versus normoxic control group; #$P < 0.01$, versus hypoxic control group; one-way ANOVA followed by Tukey's post-hoc tests

MAP4, to promote MT disruption and decrease cell viability. This suggests a link between p38/MAPK activation and Op18 dephosphorylation, which also promotes MT disruption. p38/MAPK may cause Op18 dephosphorylation through a mechanism other than direct interaction/retention (Fig. 10). Thus, future studies are required to elucidate the mechanism by which MAP4 and Op18 phosphorylation regulates MT dynamics and cell viability.

It has become increasingly clear that MAP4 can regulate the assembly-state of intracellular tubulin. In undifferentiated carcinoma cells, such as HeLa cells, MAP4 influences the MT array by modulating the level of tubulin and affecting the level of non-centrosomal MTs. MAP4 is not only critical to regulating MT dynamics during mitosis but is also involved in controlling other cellular functions, such as cell spreading and shape. In myogenic morphogenesis, Sato et al. [44] showed that heightened expression of MAP4 mRNA and protein preceded an increase in the number and stability of MTs in the myocardium undergoing hypertrophy in response to pressure overload. Previous studies by Mangan and Olmsted [45] reported that the expression of MAP4 antisense sequences in C2C12 muscle cells reduced the level of a minor, muscle-specific isoform of the MAP4 protein and compromised myogenic differentiation. Several studies have shown that the phosphorylation sites in the C-terminus proline-rich region [46] of the MT binding domains of MAP4, such as Ser696 and Ser787, are critical

sites that lead to the dissociation of MAP4 from MTs and to a pronounced increase in dynamic instability. Accordingly, we focused on the phosphorylation of a new site (Ser768) in human MAP4 (the corresponding site is predicted to be Ser738 in rats) within the proline-rich region in the MT-binding domain.

Two mechanisms have been proposed to explain the MT-destabilizing activity of Op18/stathmin. In one mechanism, Op18/stathmin forms a sequestering complex with free tubulin, in which one Op18/stathmin molecule binds two α/β-tubulin dimmers [31]. Alternatively, Op18/stathmin may increase the catastrophe frequency of MTs [32]. The MT-destabilizing activity of Op18/stathmin is turned off in response to phosphorylation on its four serine residues, Ser16, Ser25, Ser38, and Ser63 [26–29], in response to a number of signals, including those for cell proliferation and differentiation [24], since the phosphorylated form is unable to depolymerize MTs [47]. We detected the phosphorylation of Ser16 in human Op18/stathmin (corresponding site in rats is predicted to be Ser16) in this study.

Our data reveal that endogenous MAP4 is constitutively phosphorylated at low levels, while Op18/stathmin is phosphorylated at relatively high levels. However, in response to hypoxia (1% O$_2$), MAP4 phosphorylation is significantly increased but Op18/stathmin phosphorylation is decreased in CMs and HeLa cells. Phosphorylation of p38/MAPK and its activation reaches elevated levels after 15 min of hypoxia, which coincides with the increase of hypoxia-induced MAP4 phosphorylation and Op18 dephosphorylation. Both constitutive and hypoxia-induced MAP4 phosphorylation and Op18 dephosphorylation are dramatically enhanced by MKK6(Glu) overexpression and are reduced by pretreatment with the p38/MAPK inhibitor, SB203580, indicating that p38/MAPK is the major kinase responsible for phosphorylating MAP4 and dephosphorylating Op18/stathmin in these cells. We found that inhibition of p38/MAPK enhances cell viability, possibly through reduced hypoxia-induced apoptosis and its
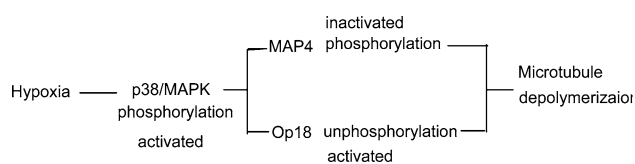

Fig. 10 A schematic representation of how hypoxia signaling promotes MT disruption. Hypoxia-activated p38/MAPK phosphorylates the downstream effector MAP4, which promotes MT disruption. It also suggests a link between p38/MAPK activation and Op18 dephosphorylation, which also promotes MT disruption. The mechanism by which p38/MAPK causes Op18 dephosphorylation and MT disruption remains unknown

inhibition of MT disruption. Conversely, overexpression of MKK6(Glu), which activates p38/MAPK, causes increased MT disruption and sensitizes cells to hypoxia-induced cell death. A pro-apoptotic effect of MKK6(Glu) expression can be correlated to increased MAP4 phosphorylation and Op18/stathmin dephosphorylation. Collectively, these findings point to a specific pathway in which p38/MAPK exerts its MT disassembly and destructive effect by phosphorylating the downstream effector MAP4 and dephosphorylating Op18/stathmin to cause MT disruption. Our results also provide evidence that there must be some other hypoxia-related mechanism(s) that also take part in hypoxia-induced MT disruption and connect p38/MAPK with Op18/stathmin dephosphorylation. It has been reported that MT and other cytoskeletal structural changes downregulated HIF-1α protein expression and its downstream proteins or signal pathways, which impaired the cell's adaptability to hypoxia [48]. Knockdown of Op18 expression suppresses HIF-1α and VEGF expression through the PI3K/AKT signaling pathway in hypoxia [49]. These discrepancies underscore the importance of understanding the physiological kinase(s) for characterizing hypoxia-induced cell physiological changes.

Recently, an increasing number of pathological conditions connected with different MT cytoskeletal changes have been reported. Disruption of the MT network has been reported in ischemia [11–13], while in some other hypoxic cardiomyopathies, such as cardiac hypertrophy [50], diabetic cardiomyopathy [51], and heart failure [52], proliferation of the MTs has been implicated in the depression of contractility. In our study, hypoxia (1% O_2 for 1 h) induced MT disruption and decreased cell viability. It raises an interesting possibility that different O_2 concentrations or amounts of time under hypoxia may induce different MT changes. We found that SB203580 had a dominant negative effect on hypoxia-induced MT disruption and increased cell viability through reduced MAP4 phosphorylation and increased Op18 phosphorylation. By comparison, overexpression studies show that p38/MAPK activation leads to a significant inhibitory effect on MT proliferation and cell viability through MAP4 phosphorylation and Op18 dephosphorylation, providing evidence supporting a pathogenic role for p38/MAPK-MAP4/Op18 phosphorylation in hypoxia. Our findings of hypoxia-induced MAP4 phosphorylation and Op18 dephosphorylation connected with the p38/MAPK pathway provides new insights into the pathogenic mechanism of MT disruption and suggests novel targets for therapeutic intervention other than MT-targeted drugs (MTDs) such as Taxol or colchicine.

In this experiment, we observed the loss of assembly MT adjacent to the cell membrane (upper panel, Fig. 1a) and the reduced stabilized population of MTs (left panel, Fig. 1b) in CMs were not as significant as those observed in HeLa cells (right panel, Fig. 1b) after hypoxia for the same time. It was reported that myocyte MTs demonstrated increased resistance to disassembly compared to the co-isolated non-myocytes [2], and the stabilized population of MTs was sufficient to maintain a normal beating rate, whereas MT dynamics (growth and shrinkage) made no observable contribution [5]. The reason for CM resistance to hypoxia-induced MT disassembly and its function need to be studied further.

References

1. Rogers SL, Gelfand VI (2000) Membrane trafficking, organelle transport, and the cytoskeleton. Curr Opin Cell Biol 12:57–62
2. Webster DR (1997) Regulation of post-translationally modified microtubule populations during neonatal cardiac development. J Mol Cell Cardiol 29:1747–1761
3. Gomez AM, Kerfant BG, Vassort G (2000) Microtubule disruption modulates Ca^{2+} signaling in rat cardiac myocytes. Circ Res 86:30–36
4. Rappaport L, Samuel JL (1998) Microtubules in cardiac myocytes. Int Rev Cytol 113:101–143
5. Webster DR, Patrick DL (2000) Beating rate of isolated neonatal cardiomyocytes is regulated by stable microtubule subset. Am J Physiol Heart Circ 278:H1653–1661
6. Yonemochi H, Saikawa T, Takakura T, Ito S, Takaki R (1990) Effects of calcium antagonists on beta-receptors of cultured cardiac myocytes isolated from neonatal rat ventricle. Circulation 81:1401–1408
7. Webster DR (2002) Microtubules in cardiac toxicity and disease. Cardiovasc Toxicol 2:75–89
8. Horwitz LD, Fennessey PV, Shikes RH, Kong Y (1994) Marked reduction in myocardial infarct size due to prolonged infusion of an antioxidant during reperfusion. Circulation 89:1792–1801
9. Hung J, Whitford EG, Parsons RW, Hillman DR (1990) Association of sleep apnoea with myocardial infarction in men. Lancet 336:261–264
10. Kyriakides ZS, Kremastinos DT, Michelakakis NA, Matsakas EP, Demovelis T, Toutouzas PK (1991) Coronary collateral circulation in coronary artery disease and systemic hypertension. Am J Cardiol 67:687–690
11. Hori M, Sato H, Kitakaze M, Iwai K, Takeda H, Inoue M, Kamada T (1994) Beta-adrenergic stimulation disassembles microtubules in neonatal rat cultured cardiomyocytes through intracellular Ca^{2+} overload. Circ Res 75:324–334
12. Hein S, Scheffold T, Schaper J (1995) Ischaemia induces early changes to cytoskeletal and contractile protein in diseased human myocardium. J Thorac Cardiov Sur 110:89–98
13. Vandroux D, Schaeffer C, Tissier C, Lalande A, Bés S, Rochette L, Athias P (2004) Microtubule alteration is an early cellular reaction to the metabolic challenge in ischemic cardiomyocytes. Mol Cell Biochem 258:99–108

14. Iwai K, Hori M, Kitabatake A, Kurihara H, Uchida K, Inoue M, Kamada T (1990) Disruption of microtubules as an early sign of irreversible ischemic injury. Immunohistochemical study of in situ canine hearts. Circ Res 67:694–706

15. Skobel E, Kammermeier H (1997) Relation between enzyme release and irreversible cell injury of the heart under the influence of the cytoskeletal modulating agents. Biochim Biophys Acta 1362:128–134

16. Sharma A, Singh M (2000) Possible mechanism of cardioprotective effect of angiotensin preconditioning in isolated rat heart. Eur J Pharmacol 406:85–92

17. Sharma A, Singh M (2000) Possible mechanism of cardioprotective effect of ischaemic preconditioning in isolated rat heart. Pharmacol Res 41:635–640

18. Sang OY, Sejeong S, Arthur MM (2005) Hypoxia stimulates carcinoma invasion by stabilizing microtubules and promoting the Rab11 trafficking of the $\alpha 6 \beta 4$ integrin. Cancer Res 7:2761–2769

19. Cassimeris L (1999) Accessory protein regulation of microtubule dynamics throughout the cell cycle. Curr Opin Cell Biol 11:134–141

20. Walczak CE (2000) Microtubule dynamics and tubulin interacting proteins. Curr Opin Cell Biol 12:52–56

21. Drewes G, Lichtenberg KB, Doring F, Mandelkow EM, Biernat J, Goris J, Doree M, Mandelkow E (1992) Mitogen activated protein (MAP) kinase transforms tau protein into an Alzheimer-like state. EMBO J 11:2131–2138

22. Ookata K, Hisanaga S, Sugita M, Okuyama A, Murofushi H, Kitazawa H, Chari S, Bulinski JC, Kishimoto T (1997) MAP4 is the in vivo substrate for CDC2 kinase in Hela cells: identification of an M-phase specific and a cell cycle-independent phosphorylation site in MAP4. Biochemistry 36:15873–15883

23. Faruki S, Karsenti E (1994) Purification of microtubule proteins from Xenopus egg extracts: identification of a 230 K MAP4-like protein. Cell Motil Cytoskeleton 28:108–118

24. Sobel A (1991) Stathmin: a relay phosphoprotein for multiple signal transduction? Trends Biochem Sci 16:301–305

25. Belmont LD, Mitchison TJ (1996) Identification of a protein that interacts with tubulin dimers and increases the catastrophe rate of microtubules. Cell 84:623–631

26. Andersen SSL, Ashford AJ, Tournebize R, Gavet O, Sobel A, Hyman AA, Karsenti E (1997) Mitotic chromatin regulates phosphorylation of stathmin/Op18. Nature 389:640–643

27. Marklund U, Brattsand G, Osterman O, Ohlsson PI, Gullberg M (1993) Multiple signal transduction pathways induce phosphorylation of serines 16, 25, and 38 of oncoprotein 18 in T lymphocytes. J Biol Chem 268:25671–25680

28. Antonson B, Lutjens R, Dipaolo G, Kassel D, Allet B, Bernard A, Catsicas S, Grenningloh G (1997) Purification, characterization and in vitro phosphorylation of the neuron-specific membrane-associated protein SCG10. Protein Expr Purif 9:363–371

29. Melander GH, Larsson N, Marklund Y, Gullberg M (1998) Regulation of microtubule dynamics by extracellular signals: cAMP-dependent protein kinase switches off the activity of oncoprotein 18 in intact cells. J Cell Biol 140:131–141

30. Andersen SS, Wittmann T (2002) Toward reconstitution of in vivo microtubule dynamics in vitro. Bioessays 24:305–307

31. Yoshinori S, Naoyuki T, Kazuyuki T, Takashi K, Yoshio Y (1997) Hypoxia and hypoxia/reoxygenation activate p65PAK, p38mitogen-activated protein kinase (MAPK), and stress-activated protein kinase (SAPK) in cultured rat cardiac myocyte. Biochem Biophys Res Commun 239:840–844

32. Florian B, Philipp S, Stephan G, Oliver H, Michael G, Ulrich K, Fleck E, Graf K (2002) Hypoxia activates β1-integrin via ERK1/2 and p38 MAP kinase in human vascular smooth muscle cells. Biochem Biophys Res Commun 296:890–896

33. Hoshi M, Ohta K, Gotoh Y, Mori A, Murofushi H, Sakai H, Nishida E (1992) Mitogen-activated-protein-kinase-catalyzed phosphorylation of microtubule-associated proteins, microtubule-associated protein 2 and microtubule-associated protein 4, induces an alteration in their function. Eur J Biochem 203:43–52

34. Birukova AA, Birukov KG, Gorshkov B, Liu F, Garcia JG, Verin AD (2005) MAP kinase in lung endothelial permeability induced by microtubule disassembly. Am J Physiol Lung C 289:75–84

35. McMillin JB, Hudson E, Buja LM (1993) Long chain acyl Co-A metabolism by mitochondrial carnitine palmitoyltransferase: a cell model for pathological studies. Methods Toxicol II:301–309

36. Seko Y, Takahashi M, Tobe K, Kadowaki T, Yazaki Y (1997) Hypoxia and hypoxia/reoxygenation activate p65(PAK), p38mitogen-activated protein kinase (MAPK), and stress-activated protein kinase (SAPK) in cultured rat cardiac myocytes. Biochem Biophys Res Commun 239:840–844

37. Joel R, Alan JW, Tamera B, Benoit D, Roger JD (1996) Mkk3- and Mkk6-regulated gene expression is mediated by the p38 mitogen-activate protein kinase signal transduction pathway. Mol Cell Bio 3:1247–1255

38. Wang Y, Krushell LA, Edelmann GM (1996) Targeted DNA recombination in vivo using an adenovirus carrying the cre recombinase. Proc Natl Acad Sci USA 93:3932–3936

39. Putnam AJ, Cunningham JJ, Dennis RG, Linderman JJ, Mooney DJ (1998) Microtubule assembly is regulated by externally applied strain in cultured smooth muscle cells. J Cell Sci 111:3379–3387

40. Takeuchi A, Mishina Y, Miyaishi O, Kojima E, Hasegawa T, Isobe K (2003) Heterozygosity with respect to zfp148 causes complete loss of fetal germ cells during mouse embryogenesis. Nat Genet 33:172–176

41. Umezu-Goto M, Kishi Y, Taira A, Hama K, Dohmae N, Takio K, Yamori T, Mills GB, Inoue K, Aoki J, Arai H (2002) Autotaxin has lysophospholipase D activity leading to tumor cell growth and motility by lysophosphatidic acid production. J Cell Biol 158:227–233

42. Brito DA, Rieder CL (2009) The ability to survive mitosis in the presence of microtubule poisons differs significantly between human nontransformed (RPE-1) and cancer (U2OS, HeLa) cells. Cell Motil Cytoskeleton 66:437–447

43. Wan X, O'Wuinn RP, Pierce HL, Joglekar AP, Gall WE, Deluca JG, Carroll CW, Liu ST, Yen TJ, McEwen BF, Stukenberg PT, Desai A, Salmon ED (2009) Protein architecture of the human kinetochore microtubule attachment site. Cell 137:672–684

44. Sato H, Nagai T, Kuppuswamy D, Narishige T, Koide M, Menick DR, Cooper G (1997) Microtubule stabilization in pressure overload cardiac hypertrophy. J Cell Biol 138:963–973

45. Mangan ME, Olmsted JB (1996) A muscle-specific variant of microtubule-associated protein 4 (MAP4) is required in myogenesis. Development 122:771–781

46. Hidefumi K, Junko I, Atsuko U, Kazu HF, Tomohiko JI, Hirokazu H, Ookata K, Murofushi H, Bulinski JC, Kishimoto T, Hisanaga S (2000) Ser787 in the proline-rich region of human MAP4 is a critical phosphorylation site that reduces its activity to promote tubulin polymerization. Cell Struct Funct 25:33–39

47. Larsson N, Marklund U, Melander GH, Brattsand G, Gullberg M (1997) Control of microtubule dynamics by oncoprotein 18: dissection of the regulatory role of multisite phosphorylation during mitosis. Mol Cell Biol 17:5530–5539

48. Escuin D, Kline ER, Giannakakou P (2005) Both microtubule-stabilizing and microtubule-destabilizing drugs inhibit hypoxia-inducible factor-1α accumulation and activity by disrupting microtubule function Cancer Res 65:9021–9028

49. Yoshie M, Miyajima E, Satoru K, Tamura K (2009) Stathmin, a microtubule regulatory protein, is associated with hypoxia-inducible factor-1α levels in human endometrial and endothelial cells. Endocrinology 150:2413–2418

50. Tsutsui H, Ishihara K, Cooper G (1993) Cytoskeletal role in the contractile dysfunction of hypertrophied myocardium. Science 260:682–687

51. Howarth FC, Quereshi MA, White E, Calaghan SC (2002) Effect of streptozotocin-induced diabetes on the cardiac microtubular cytoskeleton. Pflug Arch Eur J Physiol 444:432–437

52. Belmadani S, Pous C, Ventura CR, Fischmeister R, Mery PF (2002) Post-translational modifications of cardiac tubulin during chronic heart failure in the rat. Mol Cell Biochem 237:1141–1149